ACS APPLIED MATERIALS & INTERFACES

Research Article

www.acsami.org

Splitting a Droplet for Femtoliter Liquid Patterns and Single Cell Isolation

Huizeng Li,[†,‡,§] Qiang Yang,[†,‡,§] Guannan Li,[‡,§] Mingzhu Li,[*,‡] Shutao Wang,[‡] and Yanlin Song[*,‡]

[‡]Beijing National Laboratory for Molecular Science (BNLMS), Key Laboratory of Green Printing, Institute of Chemistry, Chinese Academy of Sciences, Beijing 100190, People's Republic of China

[§]University of Chinese Academy of Sciences, Beijing 100049, People's Republic of China

Supporting Information

ABSTRACT: Well-defined microdroplet generation has attracted great interest, which is important for the high-resolution patterning and matrix distribution for chemical reactions and biological assays. By sliding a droplet on a patterned superhydrophilic/superhydrophobic substrate, tiny microdroplet arrays low to femtoliter were achieved with uniform volume and composition. Using this method, cells were successfully isolated, resulting in a single cell array. The droplet-splitting method is facile, sample-effective, and low-cost, which will be of great potential for the development of microdroplet arrays for biological analysis as well as patterning system and devices.

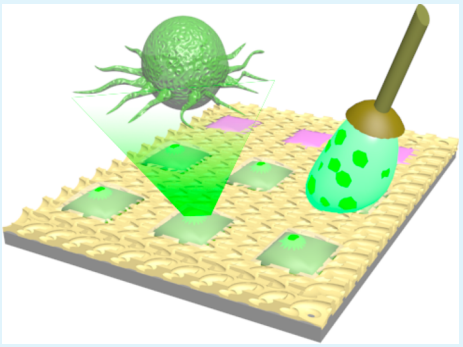

KEYWORDS: *droplet splitting, microdroplet, single cell array, superhydrophobic/superhydrophilic surface, micro/nanostructure*

INTRODUCTION

Well-defined multiple microdroplets are important in printing,[1,2] patterning,[3,4] and matrix distribution for chemical reactions and biological assays.[5−9] In these cases, it is crucial to generate and manipulate uniform microdroplets in the range from microliter to nanoliter, especially for the high-resolution printing and ultratrace quantitative assays. Plenty of methods have been employed to generate microdroplets.[10−20] For example, a superhydrophobic knife was used to split a bulk droplet into two,[10] T-junction microfluidic devices were utilized to prepare microdroplets in batch,[11−13] and high-resolution jet printing was used to produce multiple submicroliter-sized droplets through piezoelectric or electrohydrodynamic-based droplet generation.[15,16] However, most current methods were exploited for generation of microdroplets in the range of micro- and submicroliter, and to achieve nanoliter or smaller droplets, excellent-prepared or sophisticated equipment was required. It was still a great challenge to generate tiny microdroplets with controllable and uniform volume by a simple method.

Here we presented a facile strategy to split a droplet into uniform tiny microdroplet arrays with volume low to femtoliter based on the surface wettability confinement effect. By sliding a droplet on the patterned superhydrophilic/superhydrophobic substrate, homogeneous microdroplets from picoliter to femtoliter were controllably prepared. The factors key to the volume of the generated microdroplets, including the superhydrophilic pattern size, the contact force, and the relative sliding speed between the droplet and the superhydrophobic substrate, were discussed systematically. It was demonstrated that the method could provide high throughput uniform compartments that were crucial for quantitative studies, especially when the sample or reagents were expensive or limited in amount. In this study, single live cell array was achieved using the droplet-splitting method, where the cells were isolated and stuck on the superhydrophilic patterns. The droplet-splitting method was facile, sample-effective, and low-cost, which would be of great potential in the development of microdroplet arrays for biological and chemical assays, chemical reactions, and drug discovery, as well as patterning system and devices.

MATERIALS AND METHODS

Chemicals. Silver nitrate ($AgNO_3$) and fluorescein disodium salt were obtained from Sigma-Aldrich (Shanghai). 1H, 1H, 2H, 2H-perfluorodecyltrimethoxysilane (PFDTS) was obtained from J&K. The other chemicals were all obtained from Sinopharm Chemical Reagent Co., Ltd. (Beijing). And all the chemicals were used as received. Solutions were prepared with ultrapure water from a Millipore purification system (18.2 MΩ cm).

Fabrication of Superhydrophobic Substrates. Silicon wafer was cleaned with the piranha solution (H_2SO_4/H_2O_2 = 3:1). After washed with deionized water, the wafers were dipped into $HF/AgNO_3$ solution. Then the wafers were put into HNO_3 solution to remove the residual Ag on the silicon wafer. The wafers were dashed with water and dried with nitrogen. The substrates were uniformly porous with micro/nano composite structures. Then the Si plates were surface modified by chemical vapor deposition (CVD) with PFDTS.

Received: December 29, 2014
Accepted: March 12, 2015

DOI: 10.1021/am509177s
ACS Appl. Mater. Interfaces XXXX, XXX, XXX−XXX

Preparation of Superhydrophilic Patterns on the As-Prepared Superhydrophobic Substrate. The superhydrophobic substrate was covered by a photomask, and exposed under deep UV light (HW-UVX400, 400 W).

Characterization. The structure of the as-prepared substrates was investigated using scanning electron microscope (SEM, Hitachi S4800, Japan) and atomic force microscope (AFM, Bruker Multimode 8, Germany). Static contact angle (SCA) was characterized with an OCA20 instrument (Dataphysics, Germany) at ambient temperature. Adhesion force was measured using a high sensitivity micro-electromechanical balance system with a resolution of 10 μg (DataPhysics DCAT 11, Germany) and a charge-coupled-device (CCD) camera system at ambient temperature. Deionized water (Milli-Q, 18.2 MΩ cm) was employed as the source for the SCA and adhesion force measurement. The values in our contribution were the average of at least five results at different locations.

For the size of the superhydrophilic patterns was so small that characterization of the SCA and the adhesion force was conducted on the substrates prepared by UV exposure of the superhydrophobic substrates covered by a fully transparent quartz plate.

Process of Droplet Splitting. A drop of the solution of fluorescein disodium salt (10 μL, 10 μg mL^{-1}) was pinned on a homemade apparatus, and slid through the patterned substrates controlled by the facility. (Figure 6A) The relative speed was controlled by the X−Y controller of the apparatus, and the contact force was controlled by adjusting the distance between the droplet and the substrate, and displayed on a balance (Sartorius QUINTIX124−1 CN). The balance could output real-time data at a rate of 2.5−3 data per second and could be recorded by a computer. The contact force during the droplet splitting process was shown in Figures S4−S6 in the Supporting Information.

Measurement of Fluorescent Intensity. After drop splitting, the patterned substrate was stored in a 24-hole plate that was wrapped by aluminum foil, which could prevent the fluorescent molecules quenching. Fluorescent intensity measurements were performed by a microscope (Olympus, 50×) equipped with a spectrometer (Ocean Optics, Dunedin, FL, USA). All the intensities were average of at least 5 results at different patterns.

RESULTS AND DISCUSSION

Figure 1 shows the fabrication of the patterned superhydrophilic/superhydrophobic substrate (Figure 1a, b) and the controllable droplet splitting process for cells isolation (Figure 1c, d). The superhydrophobic substrate was made by electrochemical etching of the silicon wafer,[21,22] and surface modified with PFDTS. (Figure 1a). To prepare superhydrophilic patterns on the superhydrophobic substrate, the hydrophobic molecules of PFDTS were selectively removed by UV-exposure according to the designed photomask (Figure 1b). Superhydrophilic/superhydrophobic microarrays could be achieved all over the silicon wafer. The original droplet was split into multiple pico/femtoliter microdroplets by sliding the droplet through the patterned substrate (Figure 1c). With the optimized parameters, the cells in a droplet of culture medium could be isolated and resulted in a single cell array on the patterned substrate (Figure 1d).

Figure 2a, b show the surface morphology of the substrate, characterized by scanning electron microscope (SEM, Figure 2a) and atomic force microscope (AFM, Figure 2b). The open hierarchical micro/nano porous structure distributed all over the surface of the silicon wafer. The formed micro/nanostructure was essential for both the superhydrophobic and superhydrophilic properties.[23−27] The wettability of the superhydrophobic substrate and the superhydrophilic pattern was characterized by adhesion force (Figure 2c) and static contact angle (SCA, Figure 2d). The superhydrophobic substrate had an adhesion force of 0.12 ± 0.19 μN and SCA

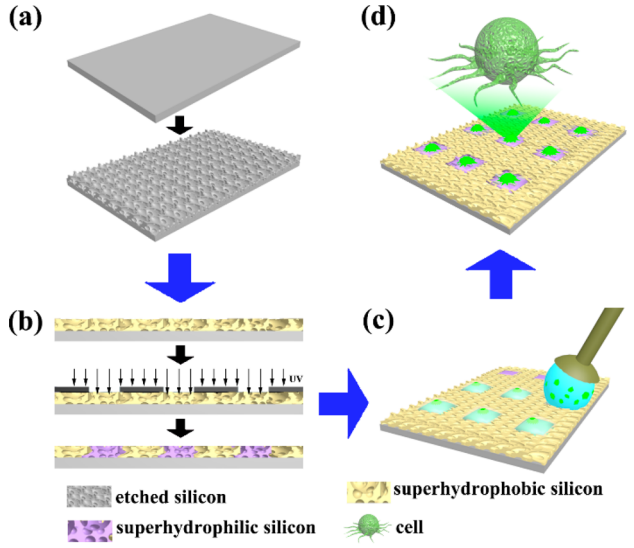

Figure 1. Schematic illustration of the process for patterned substrate preparation and application in cell isolation. (a) Preparation of the micronano composite structured silicon substrate by electrochemical etching. (b) Superhydrophilic patterns fabricated by photolithography on the superhydrophobic substrate modified with PFDTS. (c) Process of droplet splitting by sliding a droplet on the patterned substrate, resulting in submicrodroplet arrays. (d) As-prepared single cell array utilizing the droplet splitting method with a droplet of cell culture medium.

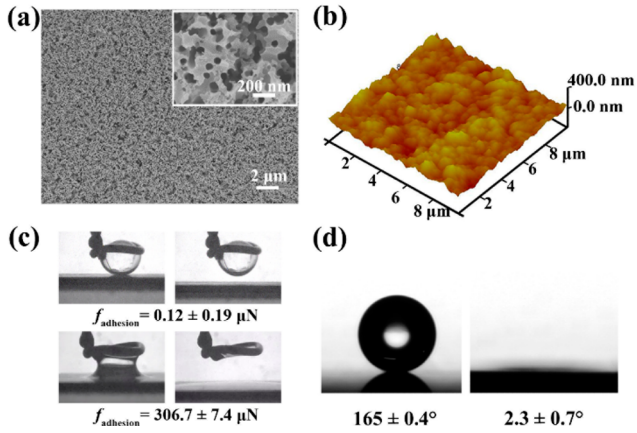

Figure 2. (a) SEM images and (b) AFM image of the porous silicon substrate after electrochemical etching. (c) Optical images of water droplets at different stages during the adhesion force measurement process of the superhydrophobic substrate (upper) and the superhydrophilic pattern (lower). (d) Static contact angles of the superhydrophobic substrate (left) and superhydrophilic pattern (right).

of 165 ± 0.4°, whereas the superhydrophilic pattern had an adhesion force of 306.7 ± 7.4 μN and SCA of 2.3 ± 0.7°. Figure 2c shows the optical images of a water droplet contacting (left) and departed from (right) the superhydrophobic substrate (upper) and the superhydrophilic substrate (lower), respectively. On the superhydrophobic substrate, no water was left after the droplet departed. In contrast, the water spread on the prepared superhydrophilic substrate. (The preparation of the superhydrophilic substrate is presented in detail in the Materials and Methods section.) For the patterned superhydrophobic/superhydrophilic substrate, the droplet was split and "stuck" on the superhydrophilic

DOI: 10.1021/am509177s
ACS Appl. Mater. Interfaces XXXX, XXX, XXX−XXX

patterns because of the surface-tension confinement (Supporting Information, Figure S1).

Superhydrophilic square patterns with different lateral length of 5, 10, 25, 50, and 100 μm were prepared on the superhydrophobic substrates. The gaps between the superhydrophilic patterns were all 200 μm. A 10 μL droplet was slid on the patterned superhydrophobic substrate, resulting in microdroplets generation. The microdroplets on those patterns were so small that most of them evaporated immediately after being split. For a visual representation of the splitting results, a solution of fluorescein disodium salt (10 μg mL^{-1}) was used, and fluorescent images of those microdroplets are shown in Figure 3a. Figure 3b shows the fluorescent intensity profiles of

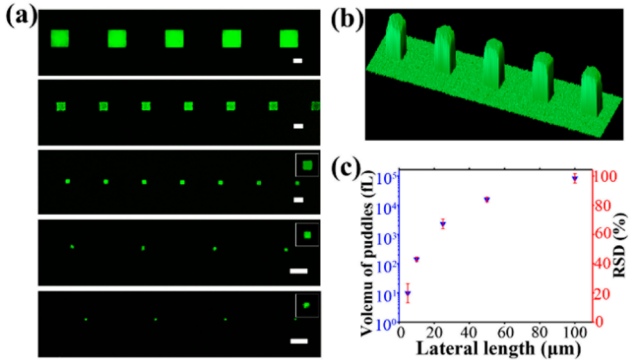

Figure 3. (a) Fluorescent images of superhydrophilic square patterns after splitting a droplet of fluorescein disodium salt solution (10 μg mL^{-1}). Lateral length was 100, 50, 25, 10, and 5 μm (scale bars 50 μm). (b) Representative fluorescent intensity profiles of five squares (100 μm lateral length, 200 μm gap). The emission intensity of the squares was homogeneous which indicated the uniformity of the as-prepared microdroplets. (c) Influence of the size of the superhydrophilic patterns on the volume of the microdroplets split from a 10 μL droplet sliding at a speed of 4 mm s^{-1} and a contact force of 200 μN.

five square patterns (100 μm lateral length, 200 μm gap) from a representative sample. The fluorescent emission of the pattern was uniform, indicating that the fluorescent molecules were uniformly distributed on the superhydrophilic areas. The relative standard deviation (RSD) of the emission intensity was smaller than 7%, which demonstrated that the volume of as-achieved microdroplets was homogeneous. Thus, the volume of the microdroplets could be characterized by fluorescent intensity (see details in the Supporting Information, page S3 and S4).

To concisely control the volume of the microdroplets, we systemically investigated the size of the superhydrophilic patterns, the contact force, and the relative sliding speed between the substrate and the original droplet. Under the same splitting conditions (sliding speed of 4 mm s^{-1} and contact force of 200 μN), a water droplet of 10 μL was slid on the substrates with patterns varied from 5 to 100 μm in lateral length. The volume of microdroplets generated increased from 9.7 fL to 83.5 pL. As shown in Figure 3c, the volume of the microdroplets increased with the increasing lateral length nonlinearly within this range.

To study the impact of the contact force between the substrate and the original droplet, we controlled a 10 μL water droplet to slide on the 100 μm patterned substrate. Relative speed was fixed at 4 mm s^{-1}, and the contact force was increased from 58.5 to 462.8 μN. Volume of the microdroplets split at different contact force ranged from 91.1 to 82.2 pL, and the relationship between the contact force and the volume of microdroplets is shown in Figure 4a. Volume of the

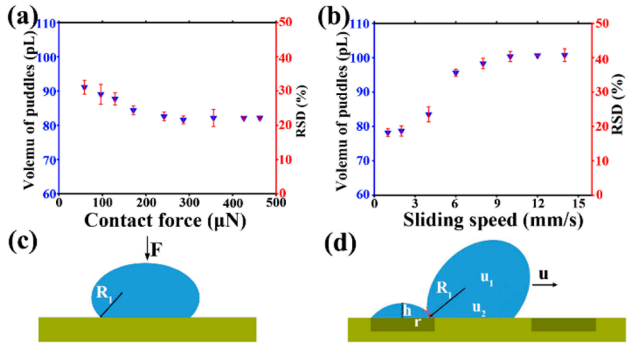

Figure 4. Effect of (a) the contact force and (b) the sliding speed on the volume of microdroplets prepared by sliding a 10 μL water droplet on 100 μm patterned substrates. (a) At a speed of 4 mm s^{-1}, the volume of the microdroplets decreased lower to 82.2 pL as the contact force increased to 260 μN, and remained unchanged at larger contact force. (b) At a contact force of 200 μN, the volume of the microdroplets prepared increased as the sliding speed increased until 10 mm s^{-1}, and then kept constant when it reached 100.7 pL. (c, d) Sketches of (c) the contact force and (d) the sliding speed between the droplet and the patterned substrate for mechanism analysis.

microdroplets decreased with increasing of contact force from 0 to 260 μN, and when the force was larger than 260 μN, the volume reached a minimum and maintained constant at the value of 82.2 pL.

To study the influence of the relative sliding speed on the volume of microdroplets, we slid a 10 μL water droplet on the 100 μm-patterned substrate. Contact force was fixed at 200 μN, and the sliding speed varied from 1 to 14 mm s^{-1}. Correspondingly, the volume of microdroplets obtained changed from 78.2 to 100.7 pL. The relationship between the volume of the microdroplet and the sliding speed is illustrated in Figure 4b. When the speed was lower than 10 mm s^{-1}, the volume increased with increasing relative speed. The microdroplets' volume reached a maximum of 100.7 pL at a speed of 10 mm s^{-1}, and remained unchanged as the speed accelerated.

To demonstrate the factors that the volume of the generated microdroplets depended on, we discussed the size of the superhydrophilic patterns, the contact force, and the relative sliding speed between the original droplet and the substrate. Geometrically, the volume of the microdroplets increased with enlarging the lateral length of patterns exponentially (see details in the Supporting Information, page S2). Influence from the contact force and the sliding speed on the volume of microdroplets on patterns of the same size was dominated by two contributors (Figure 4c, d and Supporting Information, Figure S3). One was the pressure inside the microdroplet, which consisted of capillary pressure (P_{Lm}) and shear stress (P_{sm}); the other was the capillary pressure at the receding end of the sliding droplet (P_{sd}). Pressure inside the microdroplet and at the receding end of the sliding droplet was equal

$$P_{Lm} + P_{sm} = P_{sd} \quad (1)$$

Taking Laplace Equation into account (see details of the derivation steps in Supporting Information, page S5), the relationship was represented as

DOI: 10.1021/am509177s
ACS Appl. Mater. Interfaces XXXX, XXX, XXX−XXX

$$\frac{4\gamma h}{r^2 + h^2} + \frac{\eta u}{h} = 2\gamma\frac{1}{R_1} \quad (2)$$

where R_1 was the curvature radius at the receding end of the sliding droplet, u was the sliding speed, h and r were the height and size of the microdroplet, and γ and η were the surface tension and viscosity of water, respectively. As P_{sm} was much smaller (1/1000) than P_{Lm}, P_{sm} could be omitted. Thus,

$$\frac{4\gamma h}{r^2 + h^2} = 2\gamma\frac{1}{R_1} \quad (3)$$

Under the experimental conditions, R_1 was negative correlated to h. When a force (F) performed on the static droplet, it would deform into ellipsoid. Bigger F resulted in larger R_1, which resulted in smaller h, corresponding to a smaller microdroplet. When the force increased to a certain value, R_1 of the droplet was almost infinite and stayed unchanged. Accordingly, the volume of the microdroplet would decrease first and keep unchanged afterward with increasing the contact force (Figure 4a).

When the droplet was slid on the substrate, the difference in speed ($\delta u = u_1 - u_2$) between the body component of the droplet (u_1) and the interface counterpart (u_2) would be enlarged with the sliding speed (u) increasing, resulting in smaller R_1 in the sliding droplet.[28,29] According to the analysis, smaller R_1 led to bigger h, meaning a larger microdroplet. Along with the u further accelerating, water would gather in the front of the sliding droplet, and the splitting process was completely controlled by surface tension, resulting in R_1 unchanged. Thus, the splitting capacity would remain constant. Therefore, the microdroplet-volume increased first and became plateau afterward (Figure 4b).

Quantitative particle separation on designed locations have been achieved by this simple method, which is of great importance in the field of sensing and optoelectronics.[30] As illustrated in Figure 5a, a droplet of fluorescent PS-sphere (5 μm in diameter) solution (0.6 wt %) was controlled to slide through the substrate (4 mm s^{-1}, 200 μN), leaving microdroplet arrays on the superhydrophilic patterns. After evaporation of the solvent, PS spheres were left. Figure 5b is the fluorescent image of the PS-spheres separated on the 100 μm patterns. The amount of the particles were 7, 7, 8 and 7, which was coincide well with the theoretical values (See calculations in Supporting Information, page S6), and were also demonstrated by SEM images (Supporting Information, Figure S7). The slight difference in the numbers of the PS-spheres might due to the Possion distribution. Changing the size of the superhydrophilic patterns into 50 μm, single particle array was achieved on designed locations (Figure 5c and Supporting Information, page S8).

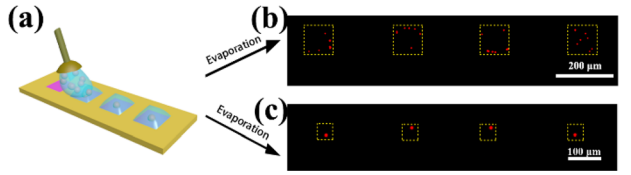

Figure 5. (a) Scheme of quantitative particle separation by splitting a droplet of PS-sphere solution on the patterned superhydrophilic/superhydrophobic substrates. (b, c) Fluorescent images of multiple and single particle arrays on the substrates with patterned size of 100 and 50 μm, respectively. The dashed-line boxes in b and c represented superhydrophilic patterns on the superhydrophobic substrate.

The method could simply generate matrix of liquid microdroplets from a single bulk droplet which would be benefit for the research on chemical microreactions and biological assays. In this work, we achieved single human breast cancer cell (MCF7) array from a 10 μL droplet of cell culture medium (concentration: 10^7 mL^{-1}, Figure 6). Recently,

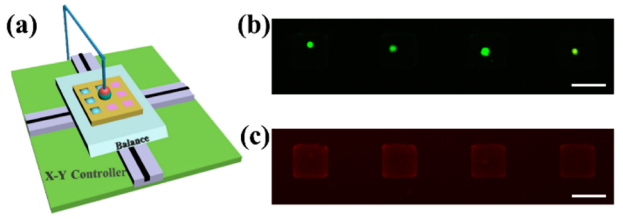

Figure 6. (a) Scheme of the homemade facility utilized to generate well-defined microdroplets. (b, c) Fluorescent images of single human breast cancer cell (MCF7) array separated by splitting a 10 μL droplet of cell culture medium (1×10^7 mL^{-1}) on superhydrophobic substrates with superhydrophilic patterns of 100 μm. The excitation wavelength of fluorescent light in (b, c) were 488 and 546 nm, respectively. Scale bars in b and c were 100 μm.

single cell isolation has attracted increasing attention across the world,[31−33] which has enormous potential in various fields, such as single cell sequencing,[34−36] cell-based detection assay,[37−39] gene and protein expression,[40,41] as well as microsensor.[42] However, it is still a challenge to separate single cell facilely from a small amount of cell culture medium. Using our droplet splitting strategy, tiny volume (10 μL, even smaller) of original solution was enough to generate hundreds of microdroplets. Cells had been stained by acridine orange/propidium iodide (AO/PI). When a 10 μL droplet of MCF7 cell culture medium was slid on the patterned superhydrophilic/superhydrophobic substrate, the cells were isolated and stuck on the superhydrophilic patterns. Single cell array was achieved on the 100 μm-patterned substrate (Figure 6b, c). The cells isolated by the superhydrophilic patterns were green under fluorescent light (488 nm), and when exposed to fluorescent light of 546 nm, the cells were almost invisible, demonstrating that single and live cell isolation had been successfully achieved. Compared with those methods that needed much more expensive and sophisticated cell isolation technologies, our strategy was low cost and facile and could be easily applied to cell assays.

CONCLUSION

In conclusion, microdroplets with controllable and uniform volume were successfully prepared by sliding a droplet on the patterned superhydrophilic/superhydrophobic substrate. Tiny microdroplets with volume ranging from 83.5 pL to 9.7 fL were successfully achieved. The volume of microdroplets could be controlled precisely by adjusting the superhydrophilic pattern size, the contact force and the relative sliding speed between the droplet and the substrate. Using this method, single cell array was successfully prepared with a droplet of cell culture medium. The presented strategy was simple, feasible and sample-effective for droplet splitting and tiny microdroplet generation. It can be anticipated that this method will yield breakthrough in the fabrication of patterned nanomaterials and optical/electrical devices, and significantly promote promising

DOI: 10.1021/am509177s
ACS Appl. Mater. Interfaces XXXX, XXX, XXX−XXX

applications in combinatorial chemistry, biological analysis, and related researches.

■ ASSOCIATED CONTENT

Supporting Information

Theoretical analysis and experimental results for calculation of microdroplets' volume; stress analysis of the droplet splitting process; theoretical calculation, fluorescent image, and SEM images of the quantitatively separated PS spheres; contact force during droplet splitting process. This material is available free of charge via the Internet at http://pubs.acs.org.

■ AUTHOR INFORMATION

Corresponding Authors

*E-mail: ylsong@iccas.ac.cn. Web site: http://ylsong.iccas.ac.cn.

*E-mail: mingzhu@iccas.ac.cn.

Author Contributions

†H.L. and Q.Y. contributed equally. The manuscript was written through contributions of all authors.

Notes

The authors declare no competing financial interest.

■ ACKNOWLEDGMENTS

M.L. and Y.S. gratefully acknowledge financial support from the 973 Program (2013CB933004, 2011CB932303, and 2011CB808400), the NSFC (Grants 51173190, 21003132, 91127038, and 21121001), Beijing Nova Program (Z131103000413051), the "Strategic Priority Research Program" of the Chinese Academy of Sciences (Grant XDA09020000), and the Chinese Academy of Sciences. We thank Dr. Pengchao Zhang for valuable discussions on cell manipulation.

■ REFERENCES

(1) Minemawari, H.; Yamada, T.; Matsui, H.; Tsutsumi, J. y.; Haas, S.; Chiba, R.; Kumai, R.; Hasegawa, T. Inkjet Printing of Single-Crystal Films. *Nature* **2011**, *475*, 364−367.

(2) de Gans, B. J.; Duineveld, P. C.; Schubert, U. S. Inkjet Printing of Polymers: State of the Art and Future Developments. *Adv. Mater.* **2004**, *16*, 203−213.

(3) Ueda, E.; Geyer, F. L.; Nedashkivska, V.; Levkin, P. A. Dropletmicroarray: Facile Formation of Arrays of Microdroplets and Hydrogel Micropads for Cell Screening Applications. *Lab Chip* **2012**, *12*, 5218−5224.

(4) Kuang, M.; Wang, L.; Song, Y. Controllable Printing Droplets for High-Resolution Patterns. *Adv. Mater.* **2014**, *26*, 6950−6958.

(5) Ziauddin, J.; Sabatini, D. M. Microarrays of Cells Expressing Defined Cdnas. *Nature* **2001**, *411*, 107−110.

(6) Hou, J.; Zhang, H.; Yang, Q.; Li, M.; Song, Y.; Jiang, L. Bio-Inspired Photonic-Crystal Microchip for Fluorescent Ultratrace Detection. *Angew. Chem., Int. Ed.* **2014**, *53*, 5791−5795.

(7) Abulikemu, M.; Da'as, E. H.; Haverinen, H.; Cha, D.; Malik, M. A.; Jabbour, G. E. In Situ Synthesis of Self-Assembled Gold Nanoparticles on Glass or Silicon Substrates through Reactive Inkjet Printing. *Angew. Chem., Int. Ed.* **2014**, *53*, 420−423.

(8) Cheng, Y.; Zhu, C.; Xie, Z.; Gu, H.; Tian, T.; Zhao, Y.; Gu, Z. Anisotropic Colloidal Crystal Particles from Microfluidics. *J. Colloid Interface Sci.* **2014**, *421*, 64−70.

(9) Chen, Z.; Hu, L.; Serpe, M. J. Liquid-Liquid Interface Assisted Synthesis of Multifunctional and Multicomponent Hydrogel Particles. *J. Mater. Chem.* **2012**, *22*, 20998−21002.

(10) Mertaniemi, H.; Jokinen, V.; Sainiemi, L.; Franssila, S.; Marmur, A.; Ikkala, O.; Ras, R. H. Superhydrophobic Tracks for Low-Friction, Guided Transport of Water Droplets. *Adv. Mater.* **2011**, *23*, 2911−2914.

(11) Song, H.; Chen, D. L.; Ismagilov, R. F. Reactions in Droplets in Microflulidic Channels. *Angew. Chem., Int. Ed.* **2006**, *45*, 7336−7356.

(12) Zhao, Y.; Shum, H. C.; Chen, H.; Adams, L. L. A.; Gu, Z.; Weitz, D. A. Microfluidic Generation of Multifunctional Quantum Dot Barcode Particles. *J. Am. Chem. Soc.* **2011**, *133*, 8790−8793.

(13) Teh, S.-Y.; Lin, R.; Hung, L.-H.; Lee, A. P. Droplet Microfluidics. *Lab Chip* **2008**, *8*, 198−220.

(14) Sakakihara, S.; Araki, S.; Iino, R.; Noji, H. A Single-Molecule Enzymatic Assay in a Directly Accessible Femtoliter Droplet Array. *Lab Chip* **2010**, *10*, 3355−3362.

(15) Ferraro, P.; Coppola, S.; Grilli, S.; Paturzo, M.; Vespini, V. Dispensing Nano-Pico Droplets and Liquid Patterning by Pyroelectrodynamic Shooting. *Nat. Nanotechnol.* **2010**, *5*, 429−435.

(16) Park, J.-U.; Hardy, M.; Kang, S. J.; Barton, K.; Adair, K.; Mukhopadhyay, D. k.; Lee, C. Y.; Strano, M. S.; Alleyne, A. G.; Georgiadis, J. G.; Ferreira, P. M.; Rogers, J. A. High-Resolution Electrohydrodynamic Jet Printing. *Nat. Mater.* **2007**, *6*, 782−789.

(17) Dong, Z.; Ma, J.; Jiang, L. Manipulating and Dispensing Micro/Nanoliter Droplets by Superhydrophobic Needle Nozzles. *ACS Nano* **2013**, *7*, 10371−10379.

(18) Jackman, R. J.; Duffy, D. C.; Ostuni, E.; Willmore, N. D.; Whitesides, G. M. Fabricating Large Arrays of Microwells with Arbitrary Dimensions and Filling Them Using Discontinuous Dewetting. *Anal. Chem.* **1998**, *70*, 2280−2287.

(19) Ostuni, E.; Chen, C. S.; Ingber, D. E.; Whitesides, G. M. Selective Deposition of Proteins and Cells in Arrays of Microwells. *Langmuir* **2001**, *17*, 2828−2834.

(20) Meyer, E.; Mueller, M.; Braun, H.-G. Preparation of Evaporation-Resistant Aqueous Microdroplet Arrays as a Model System for the Study of Molecular Order at the Liquid/Air Interface. *ACS Appl. Mater. Interfaces* **2009**, *1*, 1682−1687.

(21) Peng, K.; Lu, A.; Zhang, R.; Lee, S.-T. Motility of Metal Nanoparticles in Silicon and Induced Anisotropic Silicon Etching. *Adv. Funct. Mater.* **2008**, *18*, 3026−3035.

(22) Hu, Y.; Peng, K.-Q.; Qiao, Z.; Huang, X.; Zhang, F.-Q.; Sun, R.-N.; Meng, X.-M.; Lee, S.-T. Metal-Catalyzed Electroless Etching of Silicon in Aerated HF/H2O Vapor for Facile Fabrication of Silicon Nanostructures. *Nano Lett.* **2014**, *14*, 4212−4219.

(23) Gao, X.; Jiang, L. Biophysics: Water-Repellent Legs of Water Striders. *Nature* **2004**, *432*, 36−36.

(24) Sun, T. L.; Feng, L.; Gao, X. F.; Jiang, L. Bioinspired Surfaces with Special Wettability. *Acc. Chem. Res.* **2005**, *38*, 644−652.

(25) Feng, L.; Li, S.; Li, Y.; Li, H.; Zhang, L.; Zhai, J.; Song, Y.; Liu, B.; Jiang, L.; Zhu, D. Super-Hydrophobic Surfaces: From Natural to Artificial. *Adv. Mater.* **2002**, *14*, 1857−1860.

(26) Song, C.; Zheng, Y. Wetting-Controlled Strategies: From Theories to Bio-Inspiration. *J. Colloid Interface Sci.* **2014**, *427*, 2−14.

(27) Seo, J.; Lee, S.; Lee, J.; Lee, T. Guided Transport of Water Droplets on Superhydrophobic−Hydrophilic Patterned Si Nanowires. *ACS Appl. Mater. Interfaces* **2011**, *3*, 4722−4729.

(28) Barrer, R. M. Fluid Flow in Porous Media. *Discuss. Faraday Soc.* **1948**, *3*, 61−72.

(29) Thorsen, T.; Roberts, R. W.; Arnold, F. H.; Quake, S. R. Dynamic Pattern Formation in a Vesicle-Generating Microfluidic Device. *Phys. Rev. Lett.* **2001**, *86*, 4163−4166.

(30) Lee, M. R.; Fauchet, P. M. Nanoscale Microcavity Sensor for Single Particle Detection. *Opt. Lett.* **2007**, *32*, 3284−3286.

(31) Zhang, K.; Chou, C.-K.; Xia, X.; Hung, M.-C.; Qin, L. Block-Cell-Printing for Live Single-Cell Printing. *Proc. Natl. Acad. Sci. U.S.A.* **2014**, *111*, 2948−2953.

(32) Zhang, K.; Han, X.; Li, Y.; Li, S. Y.; Zu, Y.; Wang, Z.; Qin, L. Hand-Held and Integrated Single-Cell Pipettes. *J. Am. Chem. Soc.* **2014**, *136*, 10858−10861.

(33) Rettig, J. R.; Folch, A. Large-Scale Single-Cell Trapping and Imaging Using Microwell Arrays. *Anal. Chem.* **2005**, *77*, 5628−5634.

(34) Pennisi, E. Single-Cell Sequencing Tackles Basic and Biomedical Questions. *Science* **2012**, *336*, 976−977.

DOI: 10.1021/am509177s
ACS Appl. Mater. Interfaces XXXX, XXX, XXX−XXX

(35) Nawy, T. Single-Cell Sequencing. *Nat. Methods* **2014**, *11*, 18.
(36) Navin, N.; Hicks, J. Future Medical Applications of Single-Cell Sequencing in Cancer. *Genome Med.* **2011**, *3*, 31.
(37) Lu, G.; De Keersmaecker, H.; Su, L.; Kenens, B.; Rocha, S.; Fron, E.; Chen, C.; Van Dorpe, P.; Mizuno, H.; Hofkens, J.; Hutchison, J. A.; Uji-i, H. Live-Cell SERS Endoscopy Using Plasmonic Nanowire Waveguides. *Adv. Mater.* **2014**, *26*, 5124−5128.
(38) Lindstrom, S.; Andersson-Svahn, H. Overview of Single-Cell Analyses: Microdevices and Applications. *Lab Chip* **2010**, *10*, 3363−3372.
(39) Srisa-Art, M.; Bonzani, I. C.; Williams, A.; Stevens, M. M.; deMello, A. J.; Edel, J. B. Identification of Rare Progenitor Cells from Human Periosteal Tissue Using Droplet Microfluidics. *Analyst* **2009**, *134*, 2239−2245.
(40) Elowitz, M. B.; Levine, A. J.; Siggia, E. D.; Swain, P. S. Stochastic Gene Expression in a Single Cell. *Science* **2002**, *297*, 1183−1186.
(41) Huebner, A.; Srisa-Art, M.; Holt, D.; Abell, C.; Hollfelder, F.; Edel, J. Quantitative Detection of Protein Expression in Single Cells Using Droplet Microfluidics. *Chem. Commun.* **2007**, 1218−1220.
(42) Malinski, T.; Taha, Z. Nitric Oxide Release from a Single Cell Measured in Situ by a Porphyrinic-Based Microsensor. *Nature* **1992**, *358*, 676−678.

DOI: 10.1021/am509177s
ACS Appl. Mater. Interfaces XXXX, XXX, XXX−XXX